A Fortran 90 library for multitaper spectrum analysis ☆

G.A. Prieto [a,*], R.L. Parker [b], F.L. Vernon III [b]

[a] *Departamento de Física, Universidad de los Andes, Bogotá, Colombia*
[b] *Scripps Institution of Oceanography, University of California San Diego, La Jolla, CA 92093, USA*

ARTICLE INFO

ABSTRACT

The spectral analysis of geological and geophysical data has been a fundamental tool in understanding Earth's processes. We present a Fortran 90 library for multitaper spectrum estimation, a state-of-the-art method that has been shown to outperform the standard methods. The library goes beyond power spectrum estimation and extracts for the user more information including confidence intervals, diagnostics for single frequency periodicities, and coherence and transfer functions for multivariate problems. In addition, the sine multitaper method can also be implemented. The library presented here provides the tools needed in multiple fields of the Earth sciences for the analysis of data as evident from various examples.

© 2008 Elsevier Ltd. All rights reserved.

1. Introduction

In geosciences there is a continuing interest in the spectral analysis of various sorts of recorded or gathered data series, correlations between different series and their frequency dependence. In some cases the researcher may be interested in isolating single frequencies embedded in some noise (e.g., normal mode seismology, geological data sets, climate data) or in a continuous spectrum whose shape may be related to simple functional forms with a few parameters used to describe it (source physics, bathymetry). Another case of interest is the use of coupled data sets which can lead to the understanding of a particular problem, such as the elastic thickness using topography and gravity measurements (Simons et al., 2000), the transfer function for EM methods (Olsen, 1999; Constable and Constable, 2004), the earthquake source time function by deconvolving a record from a small earthquake from that of a larger one (Hartzell, 1978; McGuire, 2004) and recently the use of the cross-correlation between records at two seismic stations to recover the frequency-

dependent Green function between the two sites (Rickett and Claerbout, 1999; Shapiro et al., 2005; Sabra et al., 2005).

There are many articles and books focused on the subject of the estimation of the power spectral density (PSD) from finite length series. The theory and proofs of the methods used here can be found in Percival and Walden (1993). Discussion on the difficulties encountered in spectral analysis and the comparison of different methods is beyond the scope of this paper but can be found in Kay and Marple (1981), Park et al. (1987b), Bronez (1992), or Thomson (1993).

In 1982, Thomson published the seminal paper where the multitaper spectral analysis method was first presented. It has since become a classic approach, and has been applied in multiple fields in the physical sciences, medicine and economics. The multitaper method is in principle not any different to other nonparametric direct spectral estimates. The data sequence to be analyzed is multiplied by a series of weights called tapers, the result is then Fourier transformed (using an FFT) and squared to obtain the estimate of the PSD. The difference from the traditional methods such as single-taper periodograms, is that, as its name suggests, in the multitaper method a set of orthogonal tapers are used to compute many independent estimates of the PSD instead of only one. The approximately independent spectral estimates are then averaged to achieve maximum suppression of random variability. This is accomplished in traditional methods by a frequency domain smoothing.

---

* Corresponding author. Tel.: +57 1 3394949 x 4754; fax: +57 1 332 4369.
E-mail address: gprieto@uniandes.edu.co (G.A. Prieto).

There are various freely available multitaper codes (e.g., Lees and Park, 1995; Pardo-Igúzquiza et al., 1994). Various routines are also available in Matlab, R and SPlus. In this paper we present a Fortran 90 library for calculating the power spectrum of geophysical and geological time or spatial series. The advantage over previous releases of multitaper codes is that, using Fortran 90 features, additional results can be requested by the user. This means, at the users request, the library will provide not only the power spectrum, but also its confidence intervals, the complex-valued eigenspectra, and much more. In addition, proposed improvements such as Prieto et al. (2007a) or alternative methods such as the *sine multitaper* (Riedel and Sidorenko, 1995) can also be requested.

Using the Fortran library presented here it is straightforward, as we will show in some examples, to

- Obtain the PSD of a signal and the 95% confidence interval.
- Find periodic components in a background spectrum.
- Find the parameters that describe the spectrum.
- Estimate coherence and phase between two series.
- Deconvolve two series.
- Investigate polarization of signals.
- Perform time–frequency, dual-frequency analysis.
- Apply other multitaper methods (sine, quadratic).

We will present applications on some of these features using different types of data, from seismology, electromagnetics, climate, and geology to show the applicability of this library.

2. Library capabilities

This section is only intended to briefly explain the various estimates that the library can provide. The theory which it is based on can be found in detail in Percival and Walden (1993) and the references provided in each section.

2.1. Multitaper power spectrum

As mentioned in the Introduction, the data sequence is multiplied by a number of weights or tapers. These tapers (Slepian tapers) are selected to optimally minimize broad-band bias, the tendency for power from strong peaks to spread into neighboring frequency intervals of lower power (also known as spectral leakage). Each of the tapered copies of the data is Fourier transformed and a weighted average is computed to obtain a low variance result while maintaining a high-resolution estimate.

In practice only a few tapers need to be computed, depending on the resolution of the spectrum desired. The user chooses a bandwidth W over which the spectrum is smoothed, thus for an N-long sequence fixing the value NW known as the time-bandwidth product. The standard number of tapers K that need to be computed is $K = 2 * NW - 1$, although this is left for the user to decide and will depend on the particular study or type of data available.

For the kth Slepian taper v_k, we have

$$Y_k(f) = \sum_{n=0}^{N-1} y(n) v_k(n) e^{-2\pi i f n} \qquad (1)$$

the kth eigencomponent, which is the complex-valued Fourier transform of the N long data sequence $y(n)$ after being multiplied by $v_k(n)$. Here we assume unit sampling. Note that $|Y_k(f)|^2$ is a standard single-taper spectrum estimate.

Following the adaptive weighting proposed by Thomson (1982), we iteratively solve the following equations to obtain the weights d_k and the multitaper spectrum estimate $\hat{S}(f)$:

$$d_k(f) = \frac{\sqrt{\lambda_k} S(f)}{\lambda_k S(f) + (1 - \lambda_k)\sigma^2} \qquad (2)$$

where σ^2 is the variance of the signal $y(n)$, λ_k is the k eigenvalue associated with the Slepian taper v_k, and

$$\hat{S}(f) = \frac{\sum_{k=0}^{K-1} d_k^2 |Y_k(f)|^2}{\sum_{k=0}^{K-1} d_k^2} \qquad (3)$$

It is outside the scope of this paper to explain the weighting procedure. A good treatment of this topic can be found in Percival and Walden (1993) or Prieto et al. (2007b) and references therein.

2.2. Confidence intervals

Any method should provide as an essential feature both an estimate and a measure of its accuracy. Given that the statistical distributions of spectral estimators are not necessarily Gaussian (in fact the PSD is approximately χ^2 distributed) it is desirable to have confidence intervals rather than standard deviations. More about the statistics of the PSD, coherency and transfer functions for single- or multiple-taper methods can be found in Thomson and Chave (1991), Percival and Walden (1993) and Jarvis and Mitra (2001).

In the algorithm presented here we use the jackknife method to obtain confidence intervals of spectra, coherence, phase, etc. This method has the advantage that the statistical distribution of the parameter estimated does not need to be known. We follow the steps recommended in Thomson and Chave (1991), Percival and Walden (1993) and Vernon (1994). When using the sine multitaper method presented below (Section 2.5) we use the approximate known distributions for the spectrum and coherence (Jarvis and Mitra, 2001) such that the confidence limits depend on the number of tapers used to average the estimate.

These method can also be applied to obtain confidence intervals of parameters used to describe the spectrum (see for example Prieto et al., 2007b). This is the case of earthquake source physics and seafloor roughness (Goff and Jordan, 1988) where the amplitude or power spectrum is quite accurately described by a simple equation with few unknown parameters. The confidence intervals of the estimated parameters is essential here.

2.3. Test for periodic components

The study of periodic components arises in various fields including the free oscillations of the Earth (Park et al., 2005), the different modes of the Sun (p-, g-, and other modes, Thomson et al., 1995; Denison and Walden, 1999; García et al., 2007), correlation of geological data sets (ice or sediment cores) with astronomical cycles (Thomson, 1990; Park and Maasch, 1993) climate time series analysis (Chappellaz et al., 1990), etc.

Thomson (1982) proposed using the F-variance ratio to test the presence of periodic signal immersed in the background spectrum. Further discussion can be found in Percival and Walden (1993), Park et al. (1987a) and an application to the spectral reshaping (Lees, 1995) by removing the periodic components in the case where the signal of interest is the background spectrum and not the spectral lines (e.g., 60 Hz noise in instruments). The multitaper library follows the steps explained in Percival and Walden (1993) or Lees and Park (1995). Spectral reshaping can be requested by the user.

2.4. Coherence, transfer functions and deconvolution

Up to this point we have discussed algorithms for studying a single data sequence. In multivariate problems it is necessary to investigate two or more data sequences at the same time. The coherence function between gravity and topography provides relevant information about isostatic compensation mechanisms and its wavenumber dependence is related to the elastic thickness of the lithosphere (Simons et al., 2000). In seismology these codes can be used to investigate the spatial coherence of the seismic wavefield (Vernon et al., 1991). The transfer function between the external magnetic field and induced currents in Earth is also used in electromagnetism to probe the electrical conductivity in the mantle (Constable and Constable, 2004). Recently the cross-correlation (Bensen et al., 2007) or the transfer function (Saygin et al., 2006; Snieder and Safak, 2006), between records at two seismic stations have been used to retrieve the Green function between them which can later be used for seismic tomography or attenuation estimation.

It is sometimes also useful to obtain the time domain transfer function, which amounts to deconvolution. For example receiver functions are a useful tool in seismic analysis of the crust and upper mantle thicknesses (Park and Levin, 2000). In earthquake physics studies the record of a small earthquake (delta function in time and space) is assumed to represent the impulse response between the source and the receiver (Hartzell, 1978). This recorded signal can be used to deconvolve the propagation effect and provide an estimate of the source time function of the larger earthquake.

The Fortran library can estimate coherence, transfer functions and perform deconvolutions. All three algorithms are based on the cross-spectrum

$$S_{xy} = X \cdot Y^* \tag{4}$$

where X and Y are the Fourier transforms of data sequences x and y. The cross-spectrum, unlike the individual power spectra $S_x = XX^*$ or $S_y = YY^*$, is complex-valued. The magnitude squared coherence (MSC) between the two signals at a given frequency is then defined as

$$C_{xy}^2(f) = \frac{|S_{xy}(f)|^2}{S_x(f)S_y(f)} \tag{5}$$

and the transfer function is

$$T_{xy}(f) = \frac{X(f)}{Y(f)} = \frac{S_{xy}(f)}{S_y(f)} \tag{6}$$

Note that if inverse Fourier transformed T_{xy} is equivalent to deconvolution, since:

$$X(f) = Y(f) \cdot T_{xy}(f) \iff x(n) = y(n) * t(n) \tag{7}$$

where the arrow represents a Fourier transform and $t(n)$ is the time domain equivalent of T_{xy}.

The library takes advantage of the multitaper methods to add stability and remove bias. For example, in Eq. (5) if no additional averaging is performed, the MSC estimate will be unity. The use of multiple tapers provides the smoothing effect achieved by time–frequency averaging in other methods. In practice we calculate the cross-spectrum

$$\hat{S}_{xy}(f) = \sum_{k=0}^{K-1} X_k(f)Y_k^*(f) \tag{8}$$

and then the coherence

$$\hat{C}_{xy}^2(f) = \frac{|\hat{S}_{xy}(f)|^2}{\sum\limits_{k=0}^{K-1} |X_k(f)|^2 \sum\limits_{k=0}^{K-1} |Y_k(f)|^2} \tag{9}$$

and transfer function

$$\hat{T}_{xy}(f) = \frac{\hat{S}_{xy}(f)}{\sum\limits_{k=0}^{K-1} |Y_k(f)|^2} \tag{10}$$

where we have assumed $d_k = 1$, a constant weighting of the different eigencoefficients. Adding the weights d_k from Eq. (2) is straightforward. It is sometimes advantageous to add a damping factor or water-level to stabilize the transfer function estimate even further

$$\hat{T}_{xy}(f) = \frac{\hat{S}_{xy}(f)}{[\sum\limits_{k=0}^{K-1} |Y_k(f)|^2] + W_0} \tag{11}$$

although this is not being realized in the library at the moment since the choice of water-level may vary depending on the user.

2.5. Other multitaper methods

The adaptive multitaper method first introduced in Thomson (1982) had many of its characteristics designed for spectra that is locally white. In the geosciences this is not always the case and one often encounters colored spectra. In addition to the original algorithm we present also two other proposed methods that may be suitable for structured spectra. Both methods briefly described here can be applied using this library.

Riedel and Sidorenko (1995) invented the *sine multitaper* method, where instead of using the Slepian tapers a set of orthogonal sine tapers are computed. Solving a mean-square error Riedel and Sidorenko (1995) show that an optimal number of tapers can be found at each frequency. Where the spectrum is flat a large number of tapers are used, while in regions where the spectrum is structured, with peaks for example, the resolution is kept by averaging over a few tapers only.

Sine multitaper methods can sometimes reduce variance dramatically in long records where the spectrum is smooth by applying hundreds of tapers locally, something not practical with the Slepian tapers. Note, however, that this method is not recommended for high dynamic range signals (see for example Thomson et al., 2007) due to poor leakage reduction, but has the advantage of not requiring to choose a resolution bandwidth W as is needed in the original multitaper method. An additional advantage is that because the tapers are all sine functions, the Fourier transform of the original series is computed once.

In a recent publication (Prieto et al., 2007a) we suggested a refinement of the multitaper method, which we called the quadratic multitaper. By estimating the covariance matrix between the multitaper eigencomponents Y_k it is possible to calculate the derivatives of the spectrum with respect to frequency. This information is used to estimate the true curvature of the spectrum and more truthfully render the PSD function.

3. Main subroutines

3.1. `mtspec`

The multitaper library presented here has more than 50 subroutines, many of them dealing with estimating the Slepian tapers, others used to calculate the adaptive weights d_k, jackknife

error analysis, etc. There is, however, one main subroutine `mtspec` that is in charge of performing all the different steps for multitaper spectrum analysis, and there are a few individual subroutines to perform the multivariate calculations (Section 3.3) and the sine multitaper. Even the multivariate subroutines call the main routine `mtspec`.

For an adaptive multitaper spectrum estimate a basic subroutine call is

```
call mtspec ( npts,dt,x,tbp,kspec,nf,
   freq,spec )
```

where we have as inputs the number of points, sampling interval, data vector, time-bandwidth product, number of tapers, number of frequency points and as outputs the frequency and spectrum estimate vectors, respectively. These fixed parameters always need to be in the subroutine call, in that order.

One of the great advantages of Fortran 90 is the availability of *optional* arguments. The optional arguments can be added to the subroutine call, but they are not required. For example, if we type

```
call mtspec ( npts,dt,x,tbp,kspec,nf,
   freq,spec, yk=yk )
```

a npts × kspec complex array with the y_k eigencoefficients is returned. Note that the fixed parameters need to be there. Appendix A provides a more complete list of the fixed and optional arguments that can be used in calling the main subroutine.

By adding the optional argument `qispec = 1` for the subroutine call, the first two derivatives of the spectrum (Prieto et al., 2007a) are estimated and a refined multitaper spectrum estimate is returned in the output `spec`.

3.2. `sine_psd`

The subroutine call to calculate the power spectrum using the sine multitaper method (Riedel and Sidorenko, 1995) is

```
call sine_psd (npts,dt,x,ntap,ntimes,
   fact,nf, freq,spec,kopt,err)
```

where additional arguments include `ntap`, the number of tapers to use (if a constant number is requested), `ntimes`, the number of iterations for an adaptive estimation of the number of tapers, and `fact`, a smoothing factor for calculating the derivatives of the spectrum. As an additional output, the subroutine returns `kopt`, a
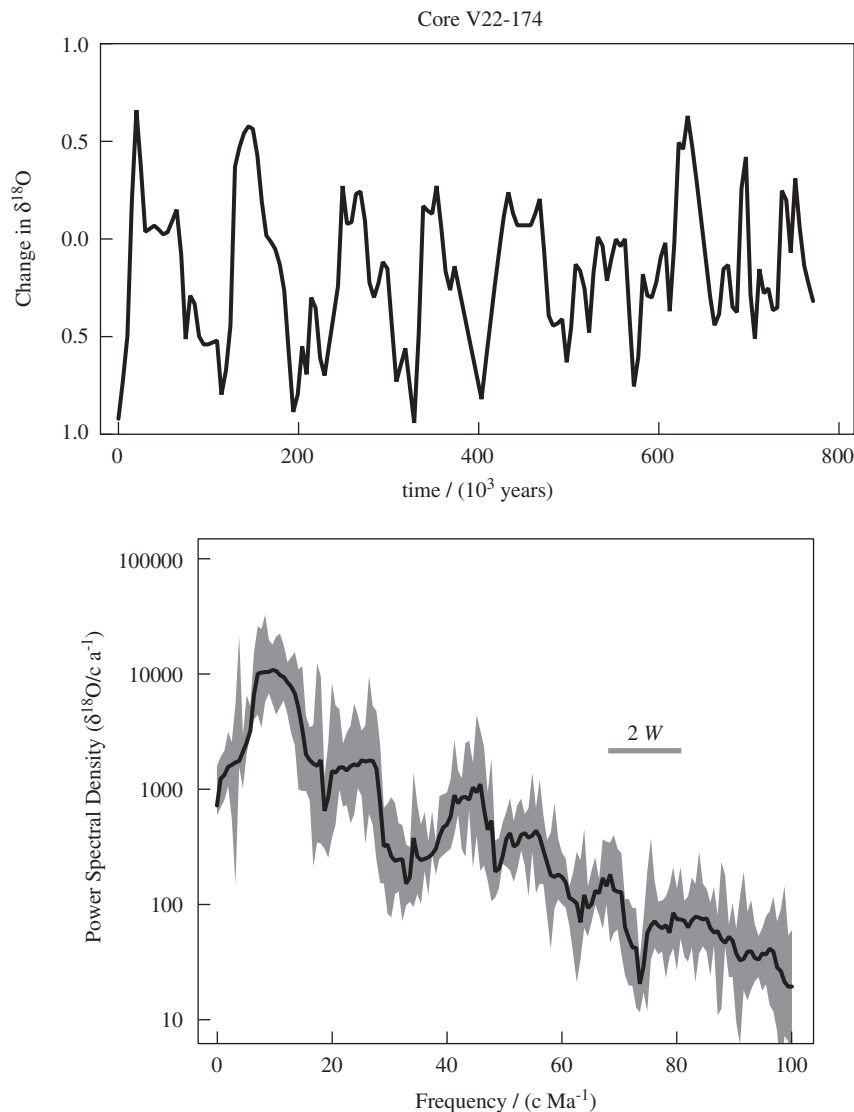

Fig. 1. δ^{18}O data from core V22-174 (top) and multitaper spectrum estimate (bottom) with 95% confidence intervals (gray shaded regions). Data have 156 samples with estimated sampling spacing of 4930 years which is padded to twice the length for the spectral estimate. A time-bandwidth product of 3.5 and 5 tapers were used.

nf long vector of integer values with the number of tapers used at each frequency bin. All arguments are needed in this case.

3.3. Multivariate subroutines

It is not the intention to describe all subroutines available in the library in this text. All subroutines have an extensive description at the beginning of each file. In this section we will list and shortly describe the subroutines to perform multivariate spectral analysis. It is assumed that the two data vectors are of the same length.

- `mt_cohe`—Coherence between two data vectors.
- `mt_transfer`—Transfer function of two data vectors.
- `mt_deconv`—Deconvolution of two data vectors.
- `sine_cohe`—Coherence using sine multitapers.

- `df_spec`—Dual-frequency spectrum of two data vectors.
- `wv_spec`—Wigner–Ville spectrum of single data vector.

4. Examples

In this section we present examples where the library can be applied for various geophysical problems. A set of simple programs are available in the distribution to allow the reproduction of the figures in the paper.

4.1. Periodic components in sediment cores

A first data set is a $\delta^{18}O$ time series from drill core V22-174 after it has been resampled for a uniform sampling interval $\Delta t = 4930$ years, taken from Thomson (1990). The time series is 156 samples long (expanding about 800 000 years). Analysis of these
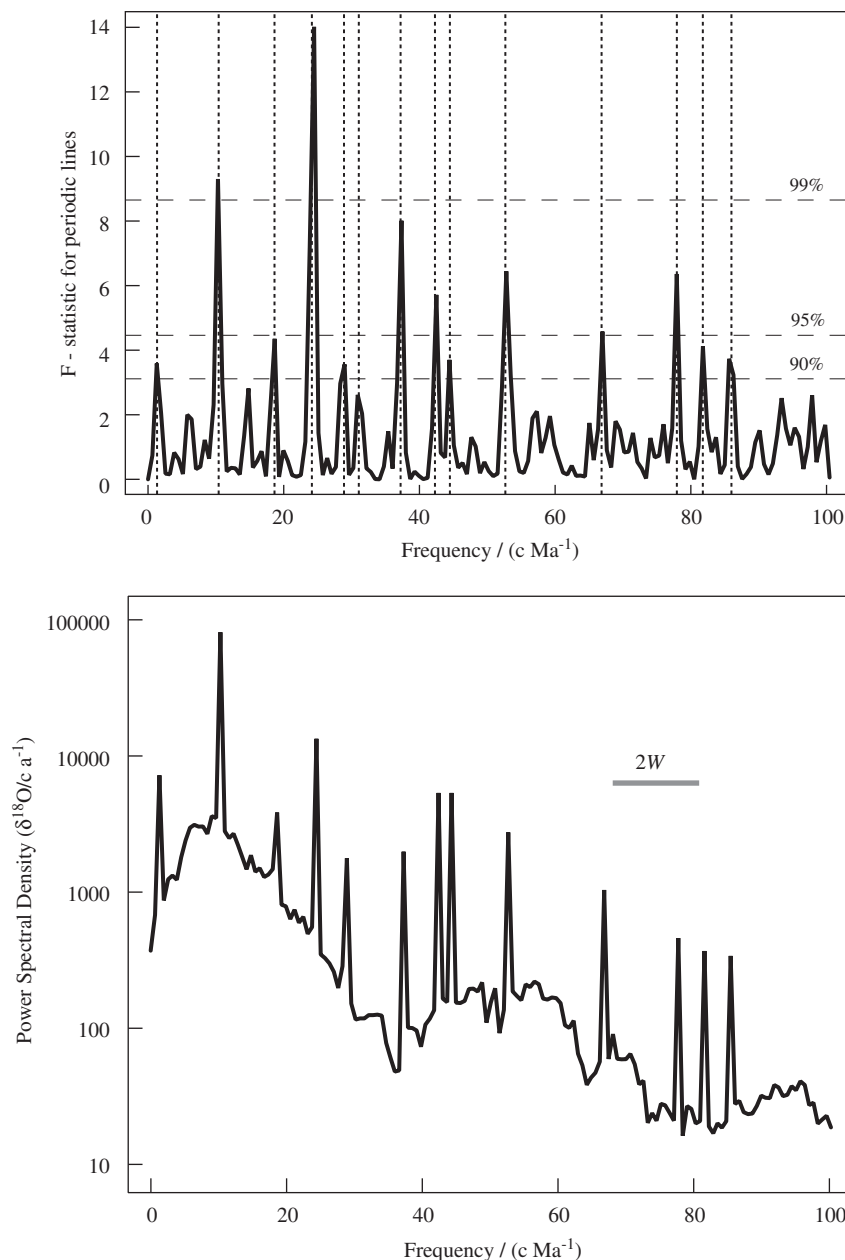

Fig. 2. *F* statistic for periodic components (top) and reshaped spectrum (bottom) with same parameters as in previous figure. Horizontal dashed lines show values where *F*-statistics exceeds the 90%, 95%, and 99% probability, which are then used in combination with results from Fig. 1 to reshape the spectrum. Vertical dotted lines show frequencies determined in Thomson (1990) for comparison.
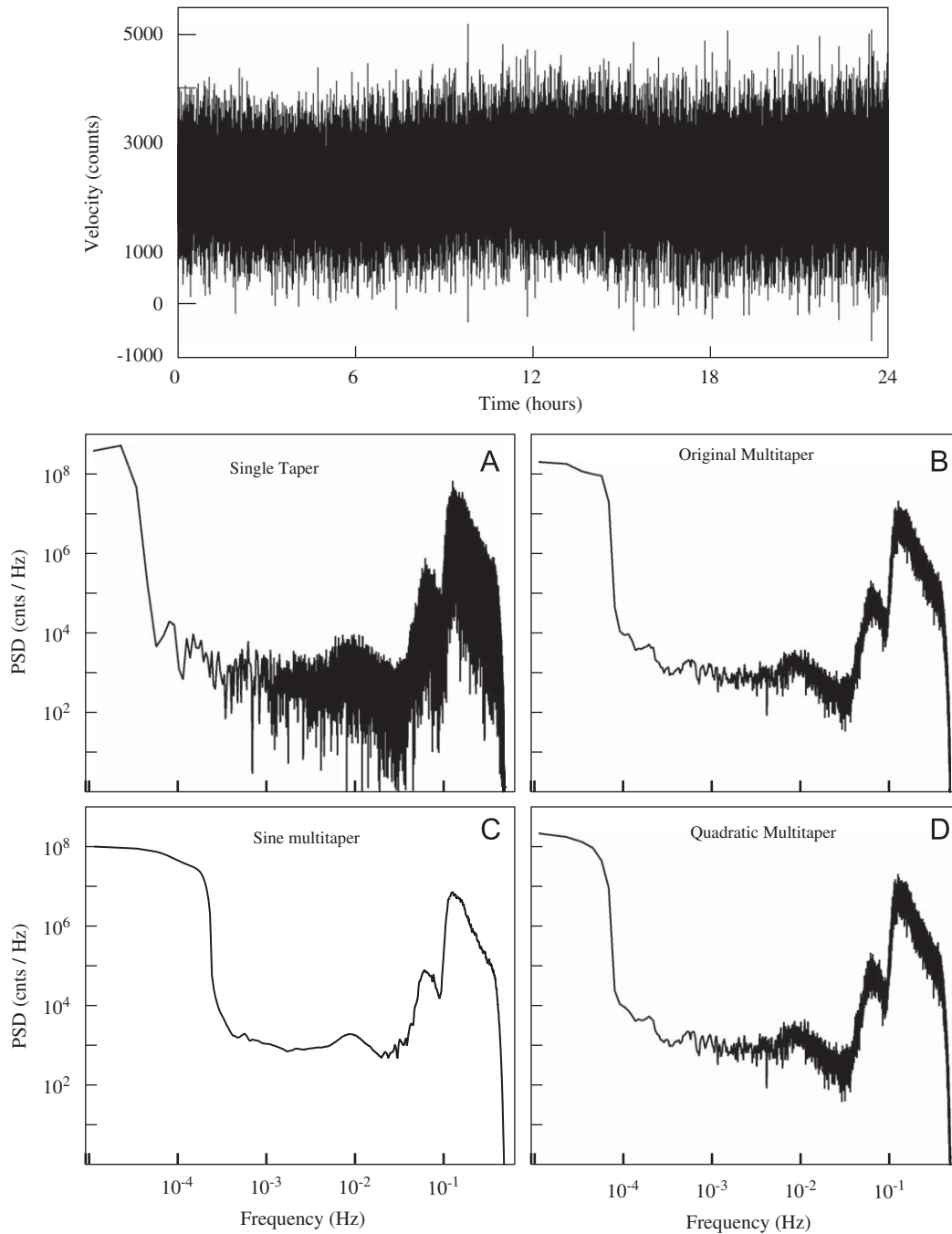
Fig. 3. Spectral analysis of a 24 hour seismic record at station PASC for January 4, 2007 without any significant earthquakes. Time series is presented in the top panel. Results for four different methods (see text for chosen parameters) are shown in lower panel. All multitaper methods provide significant reduction of variance compared to a single-taper method. Sine multitaper provides a smooth description of primary and secondary microseism peaks around 7 and 14 seconds period. At very low frequencies where a number of normal modes are expected (Earth's hum) sine multitaper may be smoothing the spectrum too much. No prewhitening is performed before calculating spectrum and no additional smoothing of spectrum is done.

kinds of time series provides relevant information about climate change in the past.

In Fig. 1 the time series δ^{18}O and a multitaper spectrum estimate with 95% confidence intervals are plotted. We use a time-bandwidth product $NW = 3.5$ and $K = 5$ tapers. The time series is padded to twice the length after tapering. Note that the spectrum estimate does not seem to have any particular periodic components. Further analysis using the F-statistics shows the presence of significant periodic components and using a 90% threshold we reshape the power spectrum with the periodic lines

in Fig. 2. The climate periodicities obtained here are similar to those presented in Thomson (1990), with some of these related to obliquity of Earth's orbit and precession of the equinoxes (Lees and Park, 1995).

4.2. Spectrum of seismic noise

The use of seismic noise has become of great interest in the last few years with the study of the source of the microseismic noise
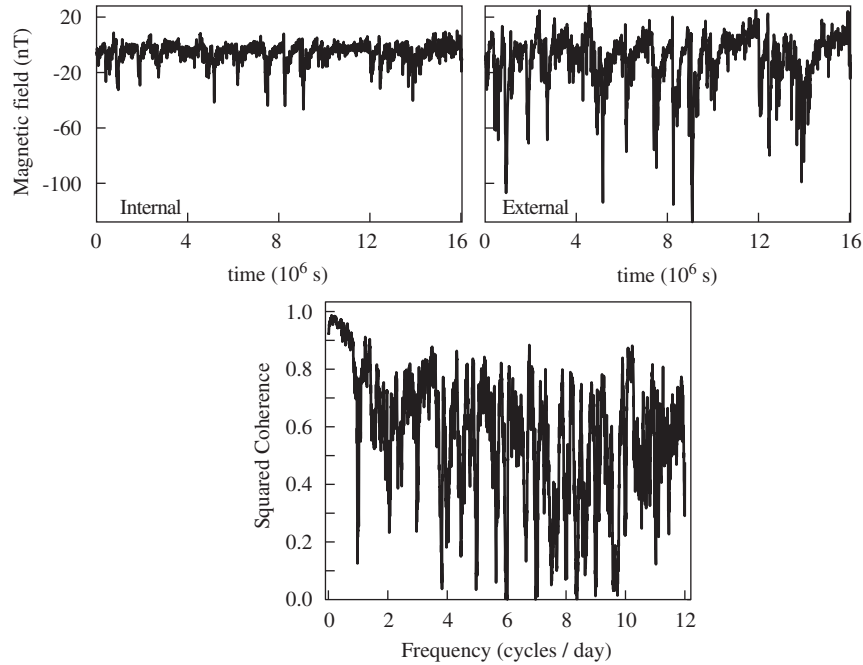
Fig. 4. Time series (top) of internal and external magnetic fields analyzed using multivariate subroutines. Data have been pre-processed in Constable and Constable (2004), for a total of 4458 sample points. Coherence between signals (bottom) shows sharp drops at harmonics of one day.

(Webb, 1998) and Earth's hum (Rhie and Romanowicz, 2004; Webb, 2007) and the use of these noise signals to retrieve Green's function between seismic stations for seismic tomography. In this example we will show a comparison of the multitaper estimates of the spectrum for a day-long record of seismic noise at the vertical component of station PASC in southern California using the standard multitaper (subroutine `mtspec`) and the sine multitaper (subroutine `sine_psd`) methods.

Fig. 3 shows a comparison of the results obtained using the algorithms presented in the library. The main objective is to show the different characteristics of the multitaper methods, while it is up to the user to decide which method is better suited for solving a particular problem. A single-taper spectrum is also shown in Fig. 3A using the first Slepian taper for a time-bandwidth of 1.5. The original 3B and quadratic multitaper 3D plots use a time-bandwidth product $NW = 4.5$ and $K = 7$ tapers. The sine multitaper adaptively using different number of tapers at each frequency.

4.3. Transfer functions in electromagnetics

Here we use the data analyzed in Constable and Constable (2004) to investigate conductivity in the Earth by looking at the frequency-dependent transfer function

$$Q(f) = \frac{i(f)}{e(f)} \tag{12}$$

where $i(f)$ and $e(f)$ are the Fourier transforms of $i_1^0(t)$ and $e_1^0(t)$, the internal and external magnetic fields, respectively (see Constable and Constable, 2004, for more details). Fig. 4 plots the two time series used, which have been resampled previously.

Using the subroutines available in this library we obtain the coherence between the two series. As discussed in Constable and Constable (2004) the coherence drops in harmonics of one day (compare to their Figure 7). The transfer function is calculated via the subroutine `mt_transfer` using a time-bandwidth product $NW = 7.5$ and $K = 12$ tapers from which we calculate the complex

admittance function

$$c = a\frac{l - (l+1)Q}{l(l+1)(1+Q)} \tag{13}$$

where a is the Earth's radius, and l is the order of the spherical harmonic function, which in this case is $l = 1$. Fig. 5 shows a comparison of our results and those using a sine multitaper method (Constable and Constable, 2004). At long periods both methods provide similar results, while at high frequencies our results differ considerably. Note that our results at short periods are closer to those of Olsen (1999) using a different data set.

4.4. Seismic noise deconvolution

As a final example we present an application of deconvolution using the multitaper library. It has been shown recently that it is possible to retrieve the Green function between two receivers by cross-correlating noisy signals (Snieder, 2004; Shapiro et al., 2005; Bardos et al., 2008). This concept has been applied to helioseismology (Rickett and Claerbout, 1999), ultrasonics (Weaver and Lobkis, 2001), seismic tomography (Bensen et al., 2007), etc. By using deconvolution instead of cross-correlations, the effect of the spectrum of the source of the noise is reduced and the convergence to the Green function is faster, as shown on applications of these methods to obtain the building response from seismic records (Snieder and Safak, 2006).

We chose recorded signals at a seismically quiet day (no significant earthquakes, as seen in Fig. 3) from stations PASC and ADO in southern California, 80 km apart. Fig. 6 shows the result of doing a cross-correlation between the day long series and performing a deconvolution using the subroutine `mt_deconv`. The results from cross-correlations are dominated by the largest amplitude of the input signals, in this case the microseism peak (see Fig. 3) at about 7 seconds period. Using a deconvolution the result has a broadband response (see inset in Fig. 6) regardless of the input signals. Note, however, that pre-processing is routinely done in noise-based tomography (Bensen et al., 2007).
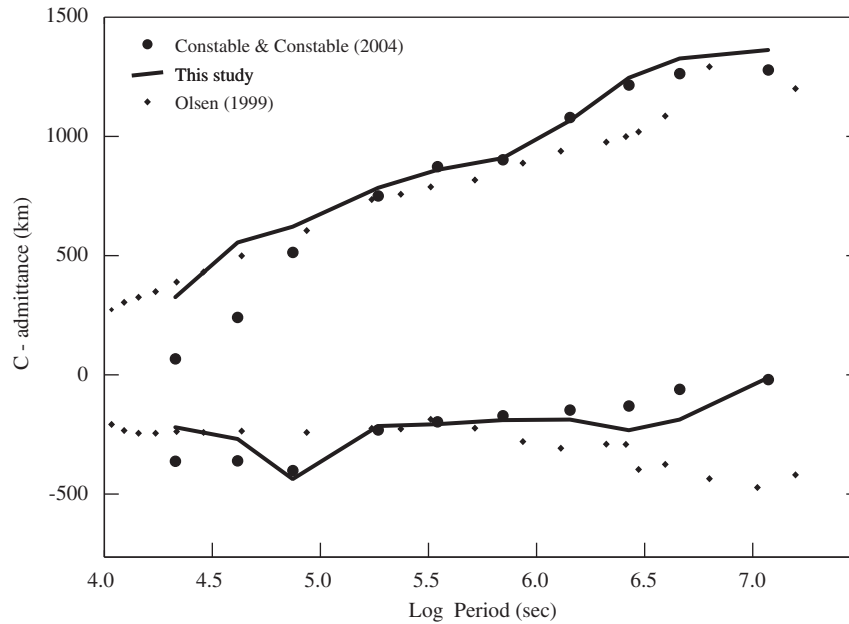
Fig. 5. Band average estimate of admittance (Eq. (13)) using multivariate subroutines. Coherence in Fig. 4 is used as a weight in band averaging the transfer function as suggested by Constable and Constable (2004). Time-bandwidth product used is $NW = 7.5$ and $K = 12$ tapers.
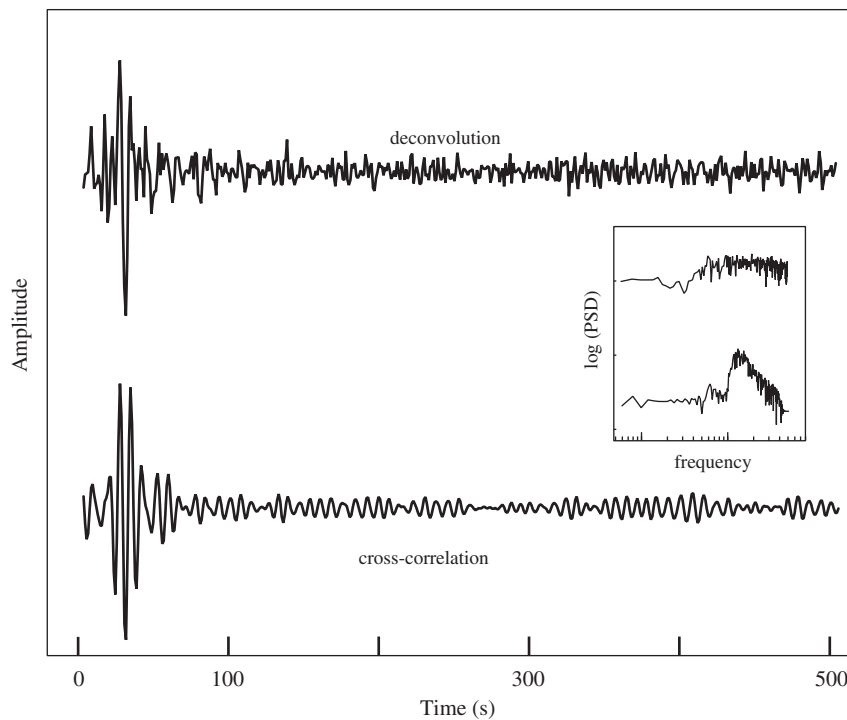

Fig. 6. Estimate of the one-sided Green's function between stations ADO and PASC in Southern California via cross-correlation and multitaper deconvolution using a day-long time series from January 4, 2007. Power spectral density of two signals is shown in inset. Cross-correlation generates a monochromatic signal evident both in time and frequency domains, while in deconvolution a broader response is obtained. No prewhitening or normalization is performed previously.

5. Interactive programs

As part of the multitaper library presented here, we created a number of interactive command-line programs for an easy to use application. The programs are in charge of loading user-specified data files (ascii files only) and calling the appropriate subroutines to perform the calculations. The user can request the results to be saved in a file and to be plotted on-the-fly.

Various parameters can be adjusted (e.g., time-bandwidth product, number of tapers, etc.) and periodic analysis, line reshaping, or using the sine multitaper method instead can be requested by the user. Other programs are included for multivariate analysis. All figures presented here (except Fig. 5 due to additional processing) can be reproduced using the interactive programs. No previous knowledge of Fortran is needed to use this programs.

6. Conclusions

The spectral analysis of geological and geophysical time series is fundamental in our understanding of Earth's processes. There are multiple methods used to extract the information from scientific data and spectral analysis and especially multitaper methods have become classic approaches. The library presented here implements the state-of-the-art multitaper analysis in an easy to use way with a large number of subroutines for doing more than just obtain a power spectrum. We present a number of examples where the library is used for spectral estimation (with error analysis), harmonic and multivariate analysis. Although beyond the scope of the paper, there are other subroutines for time–frequency analysis which can also be used. We have not discussed other applications of the multitaper methods (e.g., polarization analysis), but most of the necessary variables for doing these can be requested from the library, allowing the user to focus on the additional steps as needed.

This library is available via anonymous ftp from pangea.stanford.edu/seismo/. The distribution includes all subroutines, simple programs to replicate the figures shown in the paper and additional documentation.

Appendix A. Subroutine `mtspec` arguments

The arguments accepted in the subroutine `mtspec` are described below. Optional parameters can be requested by the user in any order, while the fixed arguments need to be given in the specific order. Table A1 provides additional characteristics of the arguments.

npts   number of points in data series
dt   sampling interval of the series

x   data vector `npts` long
tbp   time-bandwidth product desired
kspec   number of tapers to use
nf   number of frequency points in spectrum (has to be $npts/2 + 1$)
freq   frequency vector `nf` long, output
spec   PSD vector `nf` long, output
verb   verbose optional to report algorithm steps; 0—no verbose, 1—verbose (default = 0)
qispec   compute the quadratic multitaper; 0—original, 1—quadratic (default = 0)
adapt   averaging method of individual spectra; 0—adaptive, 1—constant averaging
rshape   F-test for periodic components; 0—reshape spectrum (background spectrum + lines), 1—remove line components
yk   optional output of complex-valued FFT of tapered series, `npts` long, `kspec` wide
wt   optional output of d_k weights used in estimating the spectrum, `nf` long. `kspec` wide
err   optional output with 95% confidence bounds for the spectral estimates, `nf` long, 2 columns wide
se   optional output with the degrees of freedom of the estimate, `nf` long
sk   optional output with individual single-taper estimates, `nf` long, `kspec` wide. Unnormalized
fstat   optional output with the F-statistics for periodic components, `nf` long

Table A1
Arguments accepted by main subroutine `mtspec`.

Variable	Dimension	Type	I/O	Character
npts	1	Integer	Input	Fixed
dt	1	Real	Input	Fixed
x	1	Real	Input	Fixed
tbp	1	Real	Input	Fixed
kspec	1	Integer	Input	Fixed
nf	1	Integer	Input	Fixed
freq	nf	Real	Output	Fixed
spec	nf	Real	Output	Fixed
verb	1	Integer	Input	Optional
qispec	1	Integer	Input	Optional
adapt	1	Integer	Input	Optional
rshape	1	Integer	Input	Optional
fcrit	1	Real	Input	Optional
yk	npts,kspec	Complex	Output	Optional
wt	nf,kspec	Real	Output	Optional
err	nf,2	Real	Output	Optional
se	nf	Real	Output	Optional
sk	nf,kspec	Real	Output	Optional
fstat	nf	Real	Output	Optional

References

Bardos, C., Garnier, J., Papanicolaou, G., 2008. Identification of Green's function singularities by cross correlation of noisy signals. Inverse Problems 24, 015011, (26pp).

Bensen, G.D., Ritzwoller, M.H., Barmin, M.P., Levshin, A.L., Lin, F., Moschetti, M.P., Shapiro, N.M., Yang, Y., 2007. Processing seismic ambient noise data to obtain reliable broad-band surface wave dispersion measurements. Geophysical Journal International 169, 1239–1260.

Bronez, T.P., 1992. On the performance advantage of multitaper spectral analysis. IEEE Transactions on Signal Processing 40 (12), 2941–2946.

Chappellaz, J., Barnola, J.M., Raynaud, D., Korotkevich, Y.S., Lorius, C., 1990. Ice-core record of atmospheric methane over the past 160,000 years. Nature 345, 127–131.

Constable, S., Constable, C., 2004. Observing geomagnetic induction in magnetic satellite measurements and associated implications for mantle conductivity. Geochemistry, Geophysics, Geosystems 5, Q01006.

Denison, D.G.T., Walden, A.T., 1999. The search for solar gravity-mode oscillations: an analysis using Ulysses magnetic field data. Astrophysical Journal 514, 972–978.

García, R.A., Turck-Chièze, S., Reyes, S.J.J., Ballot, J., Pallé, P.L., Eff-Darwich, A., Mathur, S., Provost, J., 2007. Tracking solar gravity modes: the dynamics of the solar core. Science 316, 1591–1593.

Goff, J.A., Jordan, T.H., 1988. Stochastic modeling of seafloor morphology: inversion of sea beam data for second-order statistics. Journal of Geophysical Research 93, 13589–13608.

Hartzell, S.H., 1978. Earthquake aftershocks as Greens functions. Geophysical Research Letters 5, 1–4.

Jarvis, M.R., Mitra, P.P., 2001. Sampling properties of the spectrum and coherency of sequences of action potentials. Neural Computation 13, 717–749.

Kay, S.M., Marple, S.L., 1981. Spectrum analysis—a modern perspective. In: Proceedings of the IEEE, vol. 69, pp. 1380–1419.

Lees, J., 1995. Reshaping spectrum estimates by removing periodic noise: application to seismic spectral ratios. Geophysical Research Letters 22 (4), 513–516.

Lees, J., Park, J., 1995. Multiple-taper spectral analysis: a stand-alone C-subroutine. Computers & Geosciences 21 (2), 199–236.

McGuire, J.J., 2004. Estimating the finite source properties of small earthquake ruptures. Bulletin of the Seismological Society of America 94, 377–393.

Olsen, N., 1999. Long-period (30 days–1 year) electromagnetic sounding and the electrical conductivity of the lower mantle beneath Europe. Geophysical Journal International 138, 179–187.

Pardo-Igúzquiza, E., Chica-Olmo, M., Rodríguez-Tovar, F.J., 1994. Cystraty: a computer program for spectral analysis of stratigraphic successions. Computers & Geosciences 20, 511–584.

Park, J., Levin, V., 2000. Receiver functions from multiple-taper spectral correlation estimates. Bulletin of the Seismological Society of America 90, 1507–1520.

Park, J., Lindberg, C.R., Thomson, D.J., 1987a. Multiple-taper spectral analysis of terrestrial free oscillations: Part I. Geophysical Journal of the Royal Astronomical Society 91, 755–794.

Park, J., Lindberg, C.R., Vernon, F.L., 1987b. Multitaper spectral analysis of high-frequency seismograms. Journal of Geophysical Research 92, 12675–12684.

Park, J., Maasch, K.A., 1993. Plio-pleistocene time evolution of the 100-kyr cycle in marine paleoclimate records. Journal of Geophysical Research 98 (B1), 447–461.

Park, J., Song, T.A., Tromp, J., Okal, E., Stein, S., Roult, G., Clevede, E., Laske, G., Kanamori, H., Davis, P., Berger, J., Braitenberg, C., Camp, M.V., Lei, X., Sun, H., Xu, H., Rosat, S., 2005. Earths free oscillations excited by the 26 December 2004 Sumatra-Andaman earthquake. Science 308, 1139–1143.

Percival, D.B., Walden, A.T., 1993. Spectral Analysis for Physical Applications: Multitaper and Conventional Univariate Techniques. Cambridge University Press, Cambridge, UK, 611pp.

Prieto, G.A., Parker, R.L., Thomson, D.J., Vernon, F.L., Graham, R.L., 2007a. Reducing the bias of multitaper spectrum estimates. Geophysical Journal International 171, 1269–1281.

Prieto, G.A., Thomson, D.J., Vernon, F.L., Shearer, P.M., Parker, R.L., 2007b. Confidence intervals for earthquake source parameters. Geophysical Journal International 168, 1227–1234.

Rhie, J., Romanowicz, B., 2004. Excitation of Earths incessant free oscillations by atmosphere–ocean–seafloor coupling. Nature 431, 552–556.

Rickett, J., Claerbout, J.F., 1999. Acoustic daylight imaging via spectral factorization: helioseismology and reservoir monitoring. The Leading Edge 18, 957–960.

Riedel, K.S., Sidorenko, A., 1995. Minimum bias multiple taper spectral estimation. IEEE Transactions on Signal Processing 43, 188–195.

Sabra, K.G., Gerstoft, P., Roux, P., Kuperman, W.A., Fehler, M.C., 2005. Surface wave tomography from microseisms in Southern California. Geophysical Research Letters 32, L14311.

Saygin, E., Kenneth, B.L.N., Reading, A.M., 2006. Exploiting ambient seismic noise—spectral broadening via transfer functions and group wavespeed tomography. Eos Transactions 87 (52) AGU Fall Meeting Supplementary Abstract S23A-0137.

Shapiro, N., Campillo, M., Stehly, L., Ritzwoller, M., 2005. High-resolution surface wave tomography from ambient seismic noise. Science 307, 1615–1618.

Simons, F.J., Zuber, M.T., Korenaga, J., 2000. Isostatic response of the Australian lithosphere: estimation of effective elastic thickness and anisotropy using multitaper spectral analysis. Journal of Geophysical Research 105 (B8), 19163–19184.

Snieder, R., 2004. Extracting the Greens function from the correlation of coda waves: a derivation based on stationary phase. Physical Review E 69, 046610.

Snieder, R., Safak, E., 2006. Extracting the building response using seismic interferometry; theory and application to the Millikan Library in Pasadena, California. Bulletin of the Seismological Society of America 96, 586–598.

Thomson, D.J., 1982. Spectrum estimation and harmonic analysis. In: Proceedings of the IEEE, vol. 70, pp. 1055–1096.

Thomson, D.J., 1990. Quadratic-Inverse spectrum estimates: applications to paleoclimatology. Philosophical Transactions of the Royal Society London A, Physical Sciences and Engineering 332, 539–597.

Thomson, D.J., 1993. Non-stationary fluctuations in "stationary" time series. In: Proceedings of the SPIE, vol. 2027, pp. 236–244.

Thomson, D.J., Chave, A.D., 1991. Jackknife error estimates for spectra, coherences, and transfer functions. In: Haykin, S. (Ed.), Advances in Spectrum Analysis and Array Processing, vol. 1. Prentice-Hall, Englewood Cliffs, NJ, pp. 58–113 (Chapter 2).

Thomson, D.J., Lanzerotti, L.J., Vernon, F.L., Lessard, M.R., Smith, L.T.P., 2007. Solar model structure of the engineering environment. In: Proceedings of the IEEE, vol. 95, pp. 1085–1132.

Thomson, D.J., Maclennan, C.G., Lanzerotti, L.J., 1995. Propagation of solar oscillations through the interplanetary medium. Nature 376, 139–144.

Vernon, F.L., 1994. Jackknifed multiple-window spectra and coherence applied to seismic data. In: Proceedings of the International Conference in Acoustic Speech and Signal Processing VI. IEEE, Adelaide, Australia, pp. 93–96.

Vernon, F.L., Fletcher, J., Haar, L., Chave, A., Sembera, E., 1991. Coherence of seismic body waves from local events as measured by a small aperture array. Journal of Geophysical Research 96, 11981–11996.

Weaver, R.L., Lobkis, O.I., 2001. Ultrasonics without a source: thermal fluctuation correlations at MHz frequencies. Physical Review Letters 87, 134301.

Webb, S.C., 1998. Broadband seismology and noise under the ocean. Reviews of Geophysics 36 (1), 105–142.

Webb, S.C., 2007. The Earth's hum is driven by ocean waves over the continental shelves. Nature 445, 754–756.